MOHAMMADALI SEPEHRI*[#], DEREK APEL*, WEI LIU*

STOPE STABILITY ASSESSMENT AND EFFECT OF HORIZONTAL TO VERTICAL STRESS RATIO ON THE YIELDING AND RELAXATION ZONES AROUND UNDERGROUND OPEN STOPES USING EMPIRICAL AND FINITE ELEMENT METHODS

OCENA STABILNOŚCI PRZODKA WYBIERKOWEGO I WPŁYW RELACJI NAPRĘŻEŃ POZIOMYCH DO PIONOWYCH NA STREFY OSIADANIA I ODPRĘŻENIA W OKOLICY PRZODKA PROWADZONEGO BEZ OBUDOWY W KOPALNIACH PODZIEMNYCH PRZY ZASTOSOWANIU METODY EMPIRYCZNEJ ORAZ METODY ELEMENTÓW SKOŃCZONYCH

Predicting the stability of open stopes can be a challenging task for underground mine engineers. For decades, the stability graph method has been used as the first step of open stope design around the world. However, there are some shortcomings with this method. For instance, the stability graph method does not account for the relaxation zones around the stopes. Another limitation of the stability graph is that this method cannot to be used to evaluate the stability of the stopes with high walls made of backfill materials. However, there are several analytical and numerical methods that can be used to overcome these limitations. In this study, both empirical and numerical methods have been used to assess the stability of an open stope located between mine levels N9225 and N9250 at Diavik diamond underground mine. It was shown that the numerical methods can be used as complementary methods along with other analytical and empirical methods to assess the stability of open stopes. A three dimensional elastoplastic finite element model was constructed using Abaqus software. In this paper a sensitivity analysis was performed to investigate the impact of the stress ratio "k" on the extent of the yielding and relaxation zones around the hangingwall and footwall of the understudy stope.

Keywords: Stability graph; Open stope design; Numerical modeling; Rock mechanics; Relaxation zone; Underground mining

Prognozowanie stabilności przodka wybierkowego stanowi poważne wyzwanie dla inżynierów górnictwa. Przez dziesięciolecia na całym świecie do projektowania przodka wybierkowego prowadzonego bez obudowy wykorzystywano metodę graficzną jako pierwszy etap prac. Jednakże metoda ta ma pewne niedogodności. Przykładowo, nie uwzględnia występowania stref odprężania wokół przodka. Innym ograniczeniem metody graficznej jest to, iż nie może być ona wykorzystana do oceny stabilności przodków

* SCHOOL OF MINING AND PETROLEUM, DEPARTMENT OF CIVIL AND ENVIRONMENTAL ENGINEERING, UNIVERSITY OF ALBERTA, EDMONTON, ALBERTA, T6G 1H9 CANADA

[#] Corresponding author: msepehri@ualberta.ca

w których ściany zawierają materiał podsadzany. Istnieją jednak metody analityczne i numeryczne, które pozwalają na przezwyciężenie tych ograniczeń. W pracy tej wykorzystano zarówno metody empiryczne jak i numeryczne do oceny stabilności przodka wybierkowego zlokalizowanego pomiędzy poziomami N9225 i N9250 w podziemnej kopalni diamentów w Diavik. Wykazano, że metody numeryczne stanowią znakomite uzupełnienie metod analitycznych i empirycznych wykorzystywanych do oceny stabilności przodków wybierkowych. Opracowano trójwymiarowy model elastyczno-plastycznych elementów skoń-czonych z wykorzystaniem oprogramowania Abaqus. W pracy tej przeprowadzono analizę wrażliwości i zbadano wpływ wskaźnika stosunku naprężeń 'k' na zasięg osiadania i powstanie stref odprężenia wokół warstw stropu i spągu w badanym przodku wybierkowym.

Słowa kluczowe: wykres stabilności, projektowanie przodka wybierkowego, modelowanie numeryczne, mechanika skał, strefa odprężona, górnictwo podziemne

1. Introduction

The assessment of the stability of open stopes is one of the critical stages in the underground mine design process. For decades, the stability graph method has been used as the first step of open stope designs around the world. The stability graph method originally developed by Mathews et al., (1981) is simple, quick and in comparison with 3D numerical modeling is much faster. This method has proven its reliability in open stope design over many years of application. However, there are some limitations with this method. First, the stability graph method does not account for the relaxation zones around the stopes. The stress factor in this method is based only on the induced compressive stress, while the relaxation zones can cause instability and dilution in many open stopes. Moreover, this method cannot be used to assess the stability of the stope surfaces made of backfill materials. This is vital in assessing the stability of secondary stopes developed using the Blasthole Stoping (BHS) method. One way to better evaluate the state of induced stress around open stopes is the use of numerical models as complementary methods along with analytical and empirical methods.

Throughout this paper, the stability of the proposed stope was evaluated using the follow-ing three steps:

First, using the modified Mathews stability graph proposed by Hadjigeorgiou et al., (1995), the stability of the proposed stope was investigated as a single mining block. In reality, the stope strike length would be divided into three mining blocks, with a strike length of less than 50 m for each block. The software packages used to estimate the *A*, *B* and *C* stability factors (i.e. stress, joint orientation and gravity adjustment factors, respectively) included Geomechanical Design Analysis (GDA; DIAS Engineering Inc., 2000) and DIPS 7.0 (Rocscience Inc., 2016).

Next, to better understanding the stress distribution around the stope blocks, a full three dimensional elastoplastic numerical model was constructed using Abaqus (ABAQUS/Standard Dassault Systemes Inc., 2012). The numerical model provides more in depth details regarding the displacement, yielding and failure zones around the proposed open stope. In addition, using this model, it is possible to predict the zone of relaxation around the surfaces of the hangingwall and footwall of each mining block.

Finally, using the developed finite element (FE) model, a sensitivity analysis was performed to investigate the impact of the horizontal stress to vertical stress ratio (*k* value) on the propaga-tion of the relaxation and yielding zones around underground openings.

1.1. Case Study: Diavik Diamond Underground Mine

The Diavik Diamond Mine is located approximately 300 kilometers northeast of Yellowknife, Northwest Territories in Canada (Fig. 1). Diavik reserves are contained in four kimberlite pipes, named as A154 North, A154 South, A148 and A21. The host rock is granite. All four pipes located under the waters of Lake Lac de Gras. The underground mining methods for the A154 North, A154 South, and A418 kimberlite pipes are Sublevel Longhole Retreat (SLR) and Blasthole Stoping (BHS). The SLR is used in the A154 South and A418 pipes. BHS is used in the A154 North pipe. The planned blasthole stopes will include primary and secondary stopes. All stopes have 7.5 m width, the strike length approximately 100 m, and height approximately 30 m sill to sill. Cemented rockfill (CRF) is to be used to backfill the stopes.
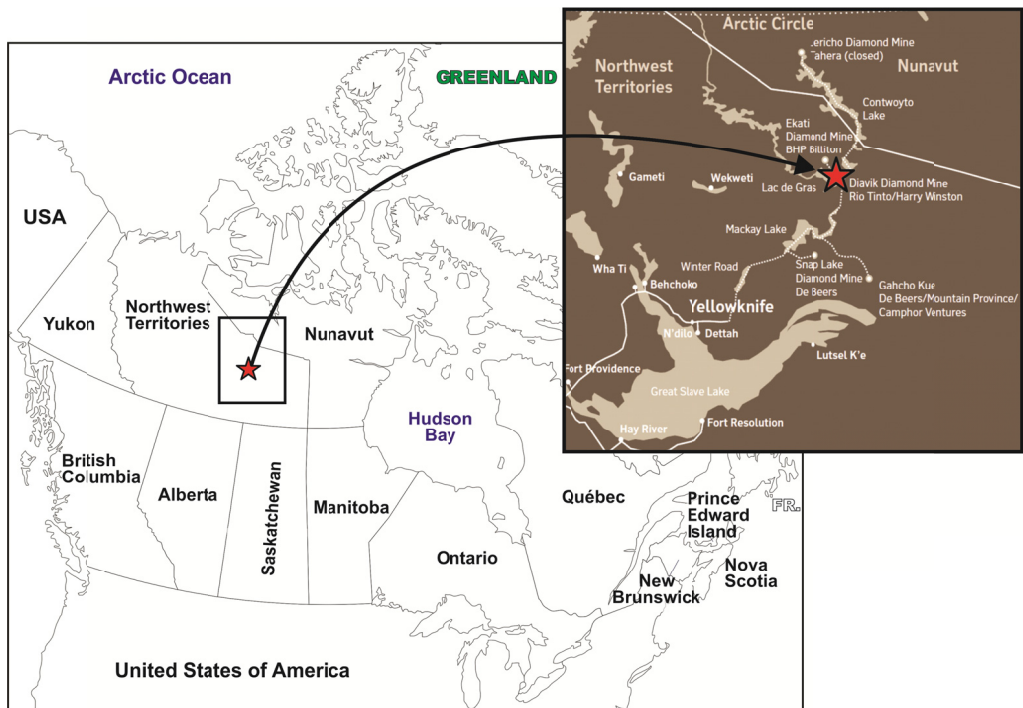

Fig. 1. Diavik Diamond Mine Location (after Diavik Dialogue, 2011)

1.2. Problem definition and objectives

The major area of concern in this paper was the assessment of the stability of a stope located at the A154 North pipe between mine levels N9225 and N9250. The understudy stope is 7.5 m wide, 30 m high and the strike length of the stope is approximately 114 m. As mentioned previously, the stope is divided into three excavation blocks, and the strike length of each block is less than 50 m. After excavation of each block, the empty stope block is backfilled immediately and excavation of the next block will be initiated.

In summary, the main objectives of this paper are: (i) to assess the stability of the proposed stope using the empirical and numerical methods; and (ii) to investigate the impact of the horizontal to vertical stress ratio on the development of yielding and relaxation zones around an underground opening.

2. Overview of the stability graph method

The stability graph method for open stope design was initially introduced by (Mathews et al., 1981) almost three decades ago. The method was modified and calibrated by (Potvin, 1988; Nickeson, 1992). The Mathews stability graph method was updated by (Stewart & Forsyth, 1995; Hadjigeorgiou et al., 1995). Today, the extended version of the method, given by (Trueman et al., 2000; Mawdesley et al., 2001), is based on more than 400 case histories collected from underground hard rock mines. A comprehensive review by (Suorineni, 2010) shows that there are some shortcomings with this method such as the need for factors that account for the stope stand-up time and blast damage. In addition, this method does not have procedures for determining the stability of stope surfaces made of backfill. Moreover, the stress factor does not account for the zones of relaxation and tension around the open stope.

The design procedure using the stability graph is based on the calculation of two parameters: N' the modified stability number, and S, the shape factor (also called the hydraulic radius, HR). Using these two parameters and the proposed graph, it is possible to estimate the stability of the understudy stope.

N' represents the ability of the rock to stand up without support under a given stress condition and is define by (Potvin, 1988) as:

$$N' = Q' \times A \times B \times C \tag{1}$$

Where Q' is the modified tunnelling quality index introduced by (Barton et al., 1974); A is the stress factor, B is the joint orientation factor, and C is the gravity adjustment factor.

HR, or S, accounts for the influence of the shape and size of the stope surface and is calculated using equation (2).

$$S = \frac{Area\,of\,the\,given\,stope\,surface}{perimeter\,\,of\,\,the\,\,stope\,surface} \tag{2}$$

3. Stability assessments using the stability graph method

The Mathews stability graph was used to determine the stability of the proposed stope. The first step was the determination of the modified stability number N' and the shape factor S for the stope surfaces. Four stope surfaces were investigated: the hangingwall, footwall, back (or roof) and vertical end-walls.

In the following sections, the modified tunnelling quality index, Q', was estimated based on the rock mass quality data, and the results are presented in table 1. The dimensions of the proposed stope block are presented in table 2. Based on the proposed dimensions, the estimated shape factor S is shown in table 3. Finally, the other stability factors (i.e. A, B, and C) were determined.

As it can be seen from table 1, two different values of Q' were estimated along the length of the stope. Therefore, the stope strike length was divided into two portions: 0 to 30 m and 30 m and 30 to 114 m. Consequently, two different N' values were calculated for the hangingwall and footwall.

TABLE 1

Value of the modified tunneling quality index

Stope surfaces	Q'
Back	5.3
Vertical end-walls	63
Hangingwall and footwall for section 1 (0-30 m of the stope length)	2.7
Hangingwall and footwall for section 2 (30-114 m of the stope length)	8.9

TABLE 2

Proposed stope dimensions

Stope Dimension		Low	High
	Length (m)	40	60
	Height (m)	30	30
	Span (m)	7.5	7.5
	Dip (°)	90	90
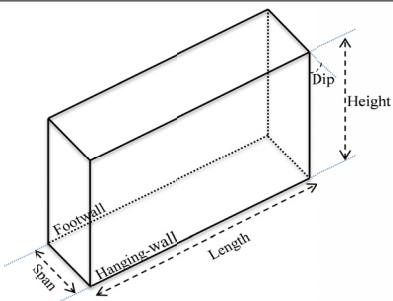
TABLE 3

Calculated shape factor (S)

Stope surface	Area (m²)		Perimeter (m)		Shape factor S (m)	
	Low	High	Low	High	Low	High
Hangingwall	1200	1800	140	180	8.57	10
Footwall	1200	1800	140	180	8.57	10
Vertical end-walls	225	225	75	75	3	3
Back	300	450	95	135	3.16	3.33

3.1. Stress factor (A)

The vertical stress was determined based on the average unit weight of the overburden rock ($\gamma = 0.026$ MN/m³). The depth of the stope is approximately 50 m. Using equation (3), the vertical stress was estimated to be 1.3 MPa.

$$\sigma_v = \gamma.H = 0.026 \times 50 = 1.3\,\text{MPa} \tag{3}$$

The unconfined compressive strength (UCS) of the kimberlite for this area was estimated to be 66 MPa. Therefore, based on the calculated vertical stress (σ_v), the value of the UCS (σ_c) and figure 2, the rock stress factor A for all stope surfaces will be 1.
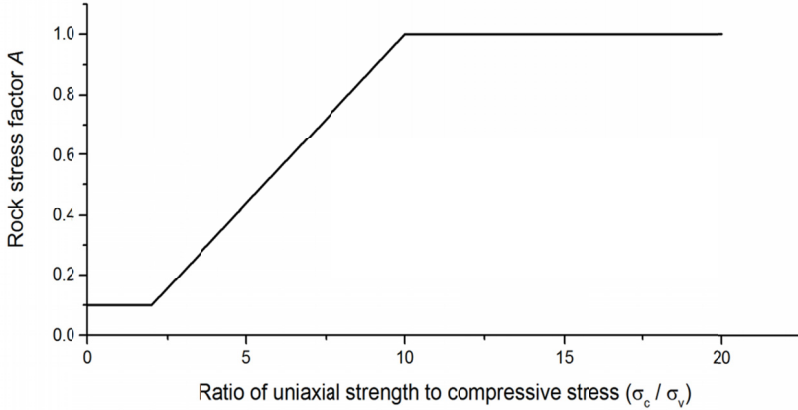

Fig. 2. Rock stress factor for different values of σc/σv (after Mathews et al., 1981)

3.2. Joint orientation factor (*B*)

Based on the site characteriziation data available for this stope, principal joints sets were defined. The dominate structure sets were determined using DIPS 7.0 (Rocscience Inc.), and the results are illustratesd in figure 3. Using the GDA software, the estiamted join orientation factors are presented in table 4.
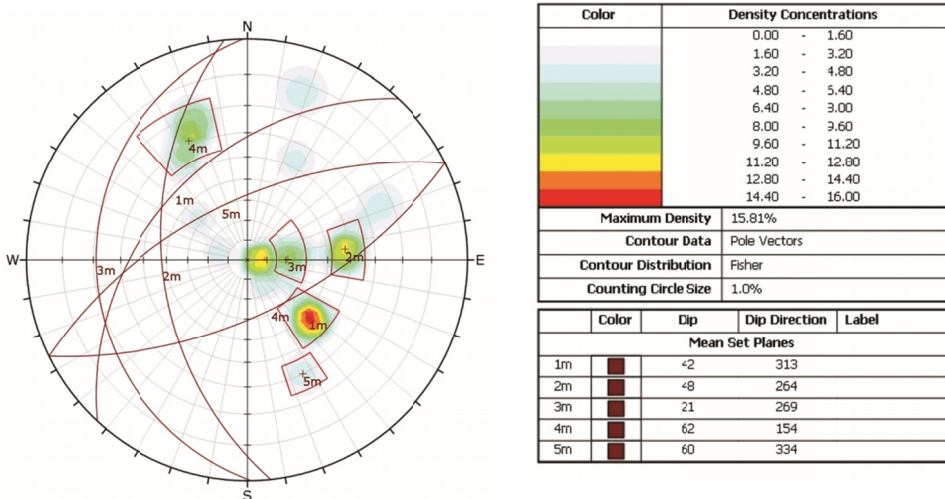

Color	Density Concentrations	
	0.00	-	1.60
	1.60	-	3.20
	3.20	-	4.80
	4.80	-	5.40
	6.40	-	3.00
	8.00	-	9.60
	9.60	-	11.20
	11.20	-	12.80
	12.80	-	14.40
	14.40	-	16.00

Maximum Density	15.81%
Contour Data	Pole Vectors
Contour Distribution	Fisher
Counting Circle Size	1.0%

	Color	Dip	Dip Direction	Label
		Mean Set Planes		
1m		‹2	313	
2m		‹8	264	
3m		21	269	
4m		62	154	
5m		60	334	

Fig. 3. The dominate structure sets

Joint orientation factor

Stope surface	Factor B
Hanging-wall	0.40
Foot-wall	0.33
Vertical endwalls	0.38
Back	0.2

3.3. Gravity adjustment factor (*C*)

This value of the gravity adjustment factor (*C)* can be estimated using equation (4), based on the inclination of each stopes surfaces (*α*). The results are presented in table 5 below.

$$\text{Factor C for gravity fall and slabbing} = 8 - 6COS(\alpha) \qquad (4)$$

Gravity adjustment factor

Stope surface	Inclination (*α°*)	Factor *C*
Hanging-wall	90	8
Foot-wall	90	8
Vertical end-walls	90	8
Back	0	2

4. Results and discussion of the stability assessment using the stability graph

4.1. Results for the first section (0 to 30 m of the stope length)

All of the stability parameters estimated for the first section of the stope length (0 to 30 m) are presented in table 6.

Stability parameters for section 1 (0-30 m)

Stope Surface	*Q'*	*A*	*B*	*C*	*N'*	*S* (m)	
						Low	High
Hanging-wall	2.7	1	0.4	8	8.66	8.57	10
Foot-wall	2.7	1	0.33	8	7.17	8.57	10
Vertical end-walls	63	1	0.38	8	190.39	3	3
Back	5.3	1	0.20	2	2.12	3.16	3.33

Based on the results presented in table 6 and using GDA software and the stability graph, the stability of the planned stope surfaces are shown in figure 4. From figure 4, the stope vertical end-walls are in the stable zone. The stope back is on the unsupported transition zone boundary.

The stope sidewalls are unstable. The sensitivity analysis for 40 to 60 m length of each stope, revealed that as the length of the stope increases the stability of the hanging-wall and foot-wall decrease. Initially, with a 40 m stope length, they are in the stable with support zone. But, as the length of the stope increases to the 60 m, they moved to the caving zone. In other words, with a 60 m strike length they are not stable even with support.
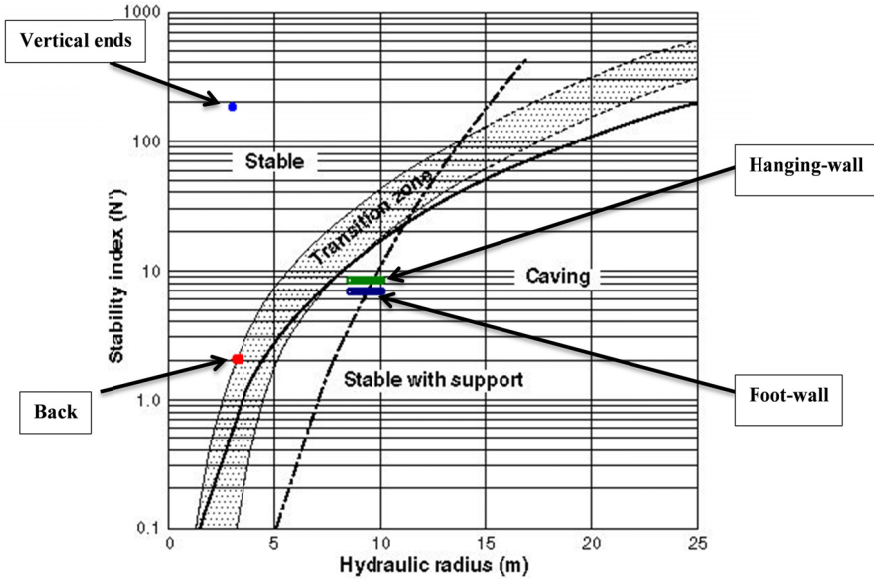

Fig. 4. Stability assessment using Mathews stability graph for section 1 using GDA software

4.2. Stability assessment for the second section (30 to 114 m of the stope length)

All of the Mathews stability parameters estimated for this section of the stope (30 to 114 m) are presented in table 7. The hangingwall and footwall in this portion of the stope have higher modified tunnelling quality index Q' values than section 1. Consequently, a larger N' value has been estimated.

TABLE 7

Stability parameters for section 2 (30 to 114 m)

Stope Surface	Q'	A	B	C	N'	S (m)	
						Low	High
Hanging-wall	8.9	1	0.4	8	28.54	8.57	10
Foot-wall	8.9	1	0.33	8	23.62	8.57	10
Vertical end-walls	63	1	0.38	8	190.39	3	3
Back	5.3	1	0.20	2	2.12	3.16	3.33

Based on the results presented in table 7 using the stability graph, the stabilities of the planned stope surfaces are estimated in figure 5.
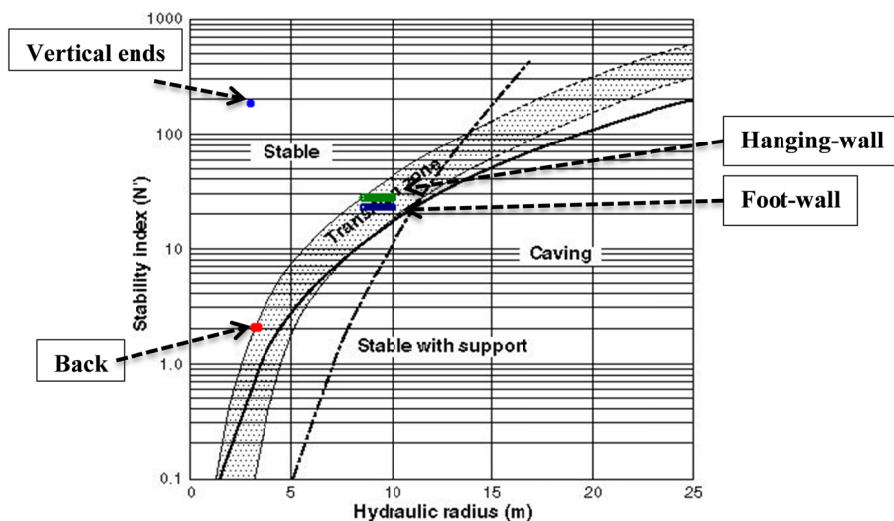

Fig. 5. Stability assessment using Mathews stability graph for section 2 using GDA software

As can be seen from figure 5, the stope vertical end-walls are in the stable zone. The stope back is on the boundary of the transition zone between stable without support and stable with support. The stope sidewalls are at the same transition zone. However, the stability of the side-walls have been improved in this section.

5. Overview of the numerical approach: finite element method

In the the last three decades, numerical methods have become popular, due to rapid advancements in computer technology. The suitability of these methods for analysis and design of very complex geotechnical problems is another reason for their popularity. Many conventional methods in rock mechanics are applicable to situations similar to the ones for which they were developed; however, there are many design problems for which no past experience is available. The finite element method (FEM) is a well-recognized numerical method which can be used for rock mechanics and geomechanical problems. It has the ability to deal with material heterogeneity, non-linearity, complex-boundary conditions, in-situ stresses and gravity.

A full three dimensional (3D) elastoplastic FE model was developed to assess the stability of the primary and secondary stopes located between mine levels N9175 to N9275 at the Diavik Diamond Mine. The FE software Abaqus (by Dassault Systems) was used to generate the FE model. In the generated model, some geometries such as the open pits were simplified such that the effective influence of the extracted pits on the in-situ stress distribution field could be captured. However, the geometries of the kimberlite pipe, undercut and overcut drifts, and the stope blocks are more representative to the actual structures.

5.1. Numerical model

A full 3D geometric representation of the mine, which is shown in Figure 6, was created based on the input data provided by the Diavik Diamond Mine. The FE model presented in this paper was also used to predict the possible subsidence on the surface due to underground mining activities. The results of these stability assessments will be presented in future publications. To accurately calculate the initial state of the stresses and to account for the zone of influence of the open pits, both A418 and A154 pits are included in the model. This allows the software to calculate the true initial state of the stresses accordingly in the first step of the simulation.
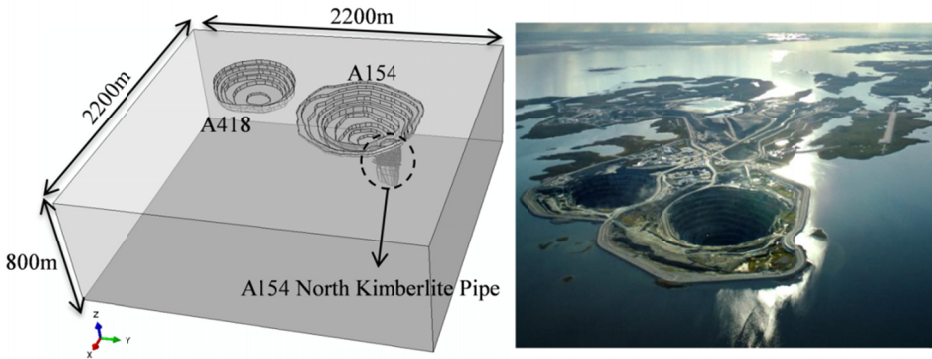

Fig. 6. Full 3D model of the mine in Abaqus (left) and aerial view of the mine

In this paper, the main focus is only on one stope: N9225-P1-185; Therefore, only the A154 North Kimberlite pipe and Mining Block A, located between mine levels N9175 and N9275 developed via BHS, are included in the model. Figure 7 shows the simplified model used for FE analysis in this paper.
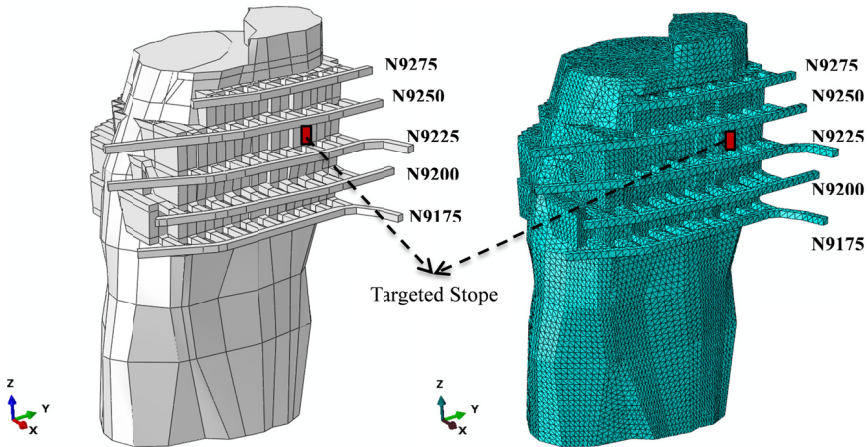

Fig. 7. Simplified model of the A154 North Kimberlite pipe and Mining Block A

In order to follow the exact sequence of mining, all primary and secondary stopes located at Mining Block A have been included in the model (Fig. 7). The geometry and the FE mesh of the P1-185 Stopes between mine levels N9175 and N9275 in the model is illustrated in figure 8. The target stope is located between mine levels N9225 and N9250. The stope is divided into three excavation blocks.
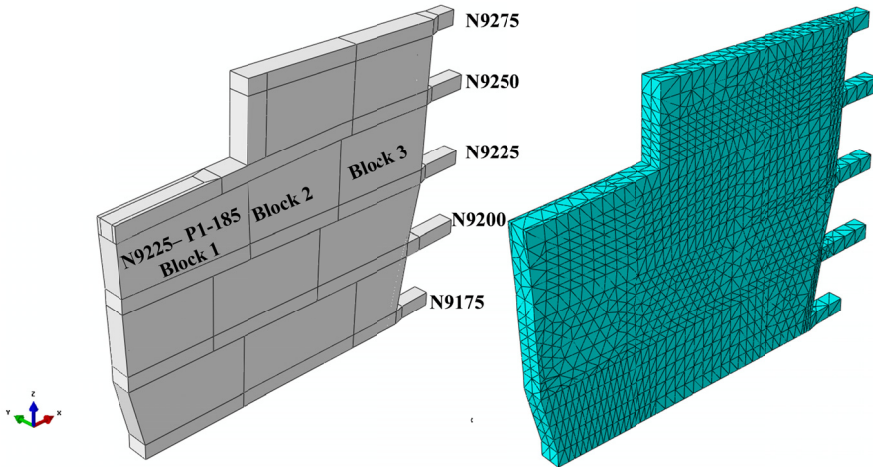

Fig. 8. Targeted stope P1 – 185 is located between mine levels N9225 and N9250

5.2. Input data assumptions and defining elements

The behavior of the rock was assumed to be governed by an elastic-plastic constitutive relation based on the elasticity theory and the Mohr-Coulomb plasticity criterion. Based on the previoue studies in the Diavik Mine, the ratio of the horizontal stress to the vertical stress (k) is assumed to be 1 in this model. The material properties used for the modeling is shown in table 8. The model has 776,794 quadratic tetrahedron elements (type C3D10), which creates 3,149,775 variables (include all degrees of freedom).

TABLE 8

Material properties

Material	Unite weight γ (MN/m³)	Elastic modulus E (GPa)	Poisson's ratio (v)	Cohesion (MPa)	Friction angle (ϕ)°	UCS (MPa)	Tensile strengh (MPa)
Granite	0.026	21	0.3	9.3	45	130	0
Kimberlite	0.026	15	0.3	1.4	42	66	0
CRF	0.022	2	0.3	1.3	35	1.5	0.2

5.3. Simulation steps

The excavation and backfilling procedures for the drifts and stopes are introduced to the model step by step. Consequently, the numerical model has 70 simulation steps. Step one is the geostatic step, which calculates the initial state of stress before starting the underground opening excavation. Step two is the excavation of five main haulage drifts between mine levels N9175 and N9275. Mining starts at mine level N9175 and going upward to N9250, through steps 3 to Step 70 of the simulation. The stope mining sequence and corresponding simulation steps are shown in figure 9.

P1 65	S2 73	P2 80	S1 88	P1 95	S2 103	P2 110	S1 118	P1 125	S2 133	P2 140	S1 148	P1 155	S2 163	P2 170	S1 178	P1 185	S2 193	P2 200	S1 208	P1 215	S2 223	P2 230	
																							N9275
						Stope																	
			55					57				60				63							N9250
										64				67								
										65				68								
										66				69								
		53		7		43		9		45		12		50		8		51		16			N9225
		61		27		50		24		47		21		55		29		58		43			
	Stope	62		28		51		25		48		22		56		30		59		44			
						52		26		49		23		57		31		60					
		44		6		31		5		32		5		33		6		47		11		62	N9200
		45		15		37		11		34		7		40		18		52		32		63	
Stope		46		16		38		12/13		35		8		41		19		53					
				17		39		14		36		9/10		42		20		54		33			
		30		4		28		3		27		3		29		4		42		10		61	N9175

Block "A" Stope Sequence:

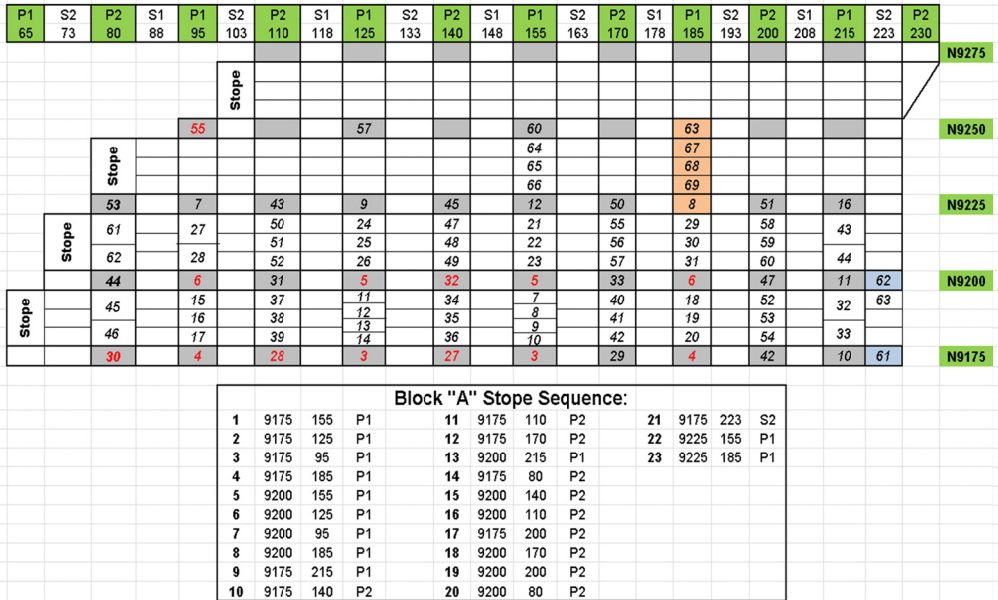|											
1	9175	155	P1	11	9175	110	P2	21	9175	223	S2
2	9175	125	P1	12	9175	170	P2	22	9225	155	P1
3	9175	95	P1	13	9200	215	P1	23	9225	185	P1
4	9175	185	P1	14	9175	80	P2				
5	9200	155	P1	15	9200	140	P2				
6	9200	125	P1	16	9200	110	P2				
7	9200	95	P1	17	9175	200	P2				
8	9200	185	P1	18	9200	170	P2				
9	9175	215	P1	19	9200	200	P2				
10	9175	140	P2	20	9200	80	P2				

Fig. 9. Mining Sequence and Simulation Steps

The stope geometry is divided into three mining blocks. In step 67, block one of the targeted stope is excavated.; step 68 is the backfilling of block one and excavation of block two of this stope; step 69 is the backfilling of block two and excavation of block 3; and step 70 is the backfilling of block 3.

6. Results and discussion of the stability assessments using numerical model

During this study, the stability of each mining block of a targeted stope was investigated. The main areas of interset were the stability of the hangingwall, footwall, vartical end-walls and the back of each excavation block of the targeted stope. To assess the stability of the understudy stope, two criteria were used: (i) yielding zones; and (ii) relaxation zones

6.1. Yielding zones

In this study, it was assumed that the behavior of the rock is elastoplastic. The Mohr-Coulomb yield function with non-associated flow rule was used. In geomechanics problems, the yielding zones can have great impact on the developing instability. Based on the reults of the FE model, there were no significant yielding zones around each stope block, except around the Kimberlite vertical wall of Block 2 shown in figure 10.
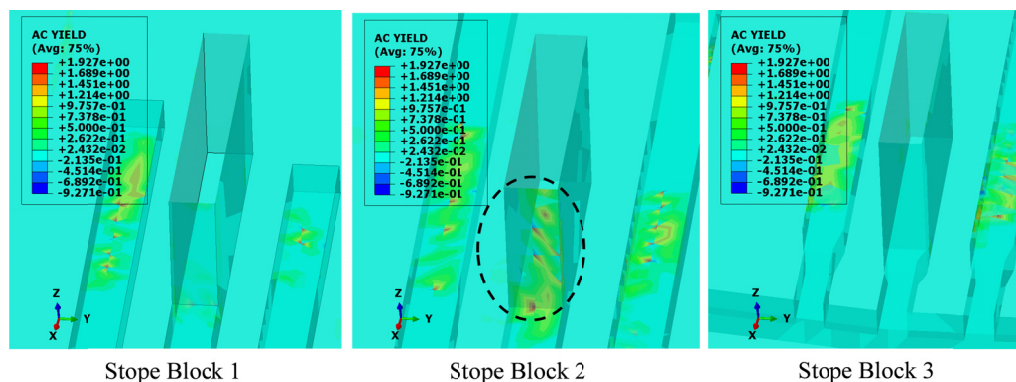

Fig. 10. Yielding zones around each stope block

6.2. Relaxation zones

One of the important factors that can influence the stability of an underground opening is the relaxation zone or tensile stress zone. According to Potvin (1988), because there is no confinement around this zone, individual rock blocks have more freedom to move. Therefore, under the influence of the gravitational forces, there is a high potential for instability and unplanned dilution. The relaxation zones around each stopes blocks are shown in figure 11. A significant development of the relaxation zone around Block 3 is illustrated in figure 12.

6.3. Sensitivity analysis

To investigate the effect of the k value (the ratio of the horizontal stress to vertical stress) on the stability of the open stope, sensitivity analysis was performed. Seven heterogeneity stress regimes with different k values ranging from 0.33 to 1.6 were assumed. In this study, the influence of stress regime on the relaxation zone and yielding zones were quantified. The main model was simplified and concentrated only on the targeted stope.

6.3.1. Yielding zone

The extent of the yielding zones around Block 1 of the understudy stope, under different k value situations, are illustrated in figure 13. Five different in-situ stress regimes were investigated. As the k value increases, the yielding zones around the opening extended significantly. When the k value is 2, the yielding zone reaches the N9290 bench surface.
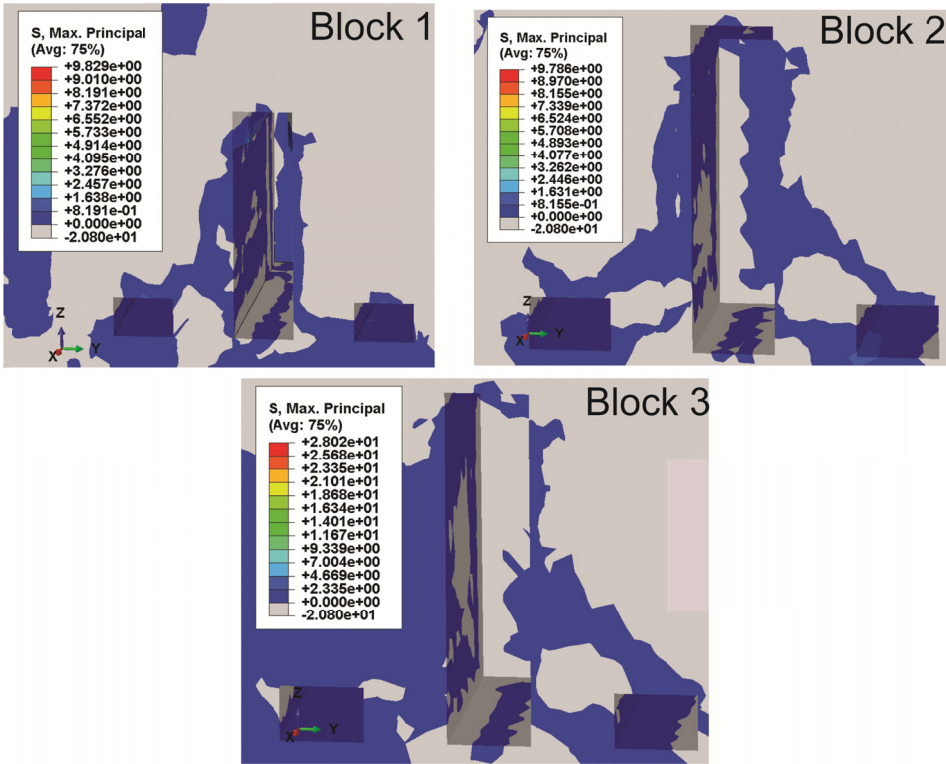
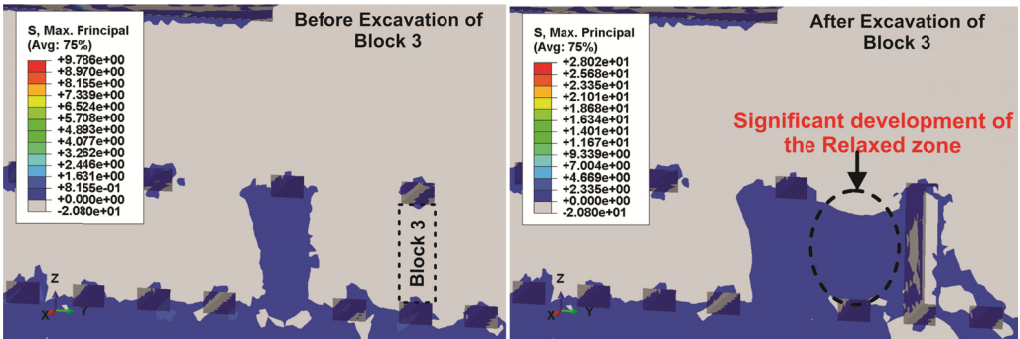Fig. 11. Relaxation zones around each stope block

Fig. 12. Development of the relaxed zone after excavation of Stope Block 3

6.3.2. Relaxation zones

To investigate the impact of the stress regime on the relaxation zone, seven different stress regimes were examined. The average relaxation depth around stope Block 2 was recorded under different stress regimes. The results are presented in figures 14 and 15.
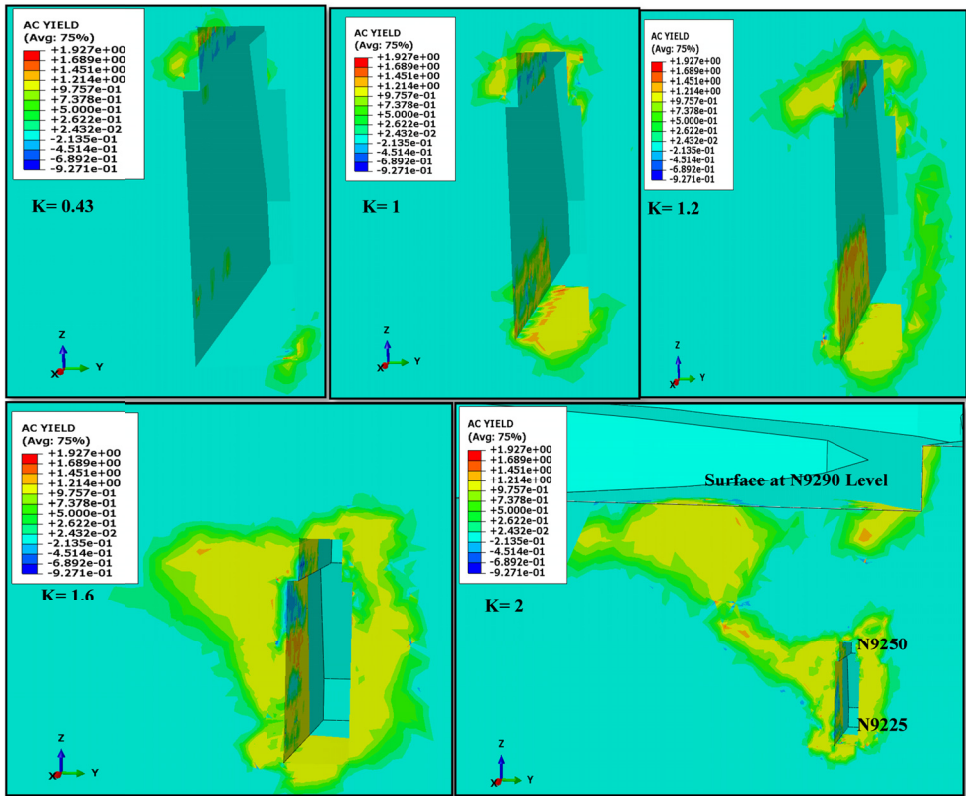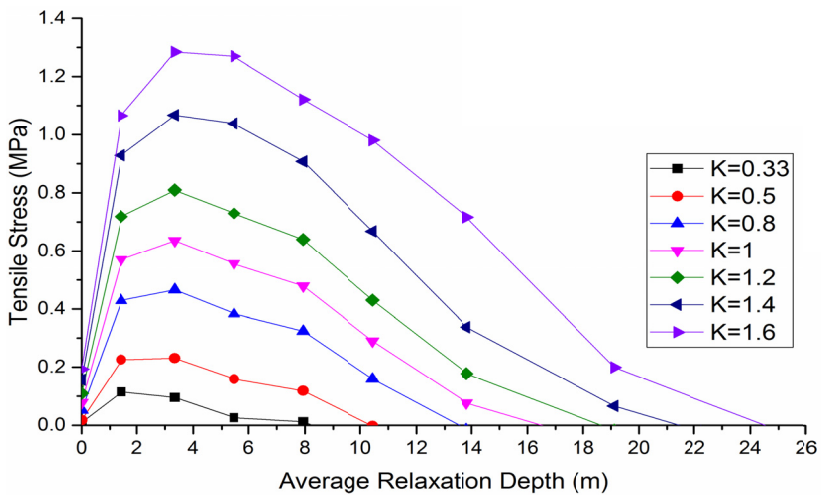
Fig. 13. The extend of the yielding zones around Block 1 with different k value

Fig. 14. Average relaxation depth (ARD) and magnitude of the tensile stresses under different stress regimes
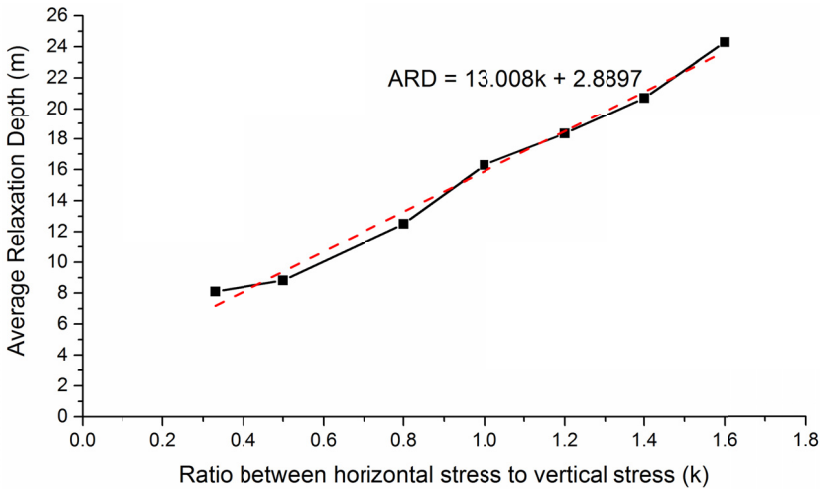
Fig. 15. Average relaxation depth (ARD) for different stress regimes

From figures 14 and 15, as the *k* value increases, not only the magnitude of the tensile stress increases but also the average relaxation depth (ARD) increases significantly. The tradeline for the average relaxation depth around the under study stope corresponds to equation (5) below:

$$ARD = 13.008\,k + 2.8897 \qquad (5)$$

7. Conclusions

The numerical model generated in this study was based on the assumption that the rock mass is continuous. By introducing the discontinuities and joint sets into the model, more accurate results can be obtained.

Throughout this paper, two underground stability assessment methods (one empirical and one numerical) were used. The main objective was to estimate the stability of a targeted stope located between mine levels N9250 and N9225 at Diavik Mine. A sensitivity analysis was also performed to investigate the effect of the stress ratio, *k*, on the development of the relaxation zones and the yielding zones around the underground stope walls. Overall the following conclusions can be drawn from this study:

- The numerical model provides better understanding of the stress distribution around the stope side walls. Particularly, the de-stressed area around the hanging-wall and foot-wall of each stope block can be estimated accurately. Having a better understanding of this de-stressed area can help identify possible zones of tensile stress. For instance, the depth of the relaxation zone can be easily identified in the numerical model. In addition, it can provide assistance when correcting the ground support design parameters (i.e. the length of the rock bolts or cable bolts).
- Based on the results of this study, the ratio between horizontal stress to vertical stress (*k* value) has a significant impact on the development and propagation of the relaxation and yielding zones around underground openings

- Since the *k* value is an uncertain parameter in most underground mines, results of this sensitivity analysis can be used to further the risk analysis associated with the stability of the stope.

Acknowledgment

References

Barton N., Lien R., Lunde J., 1974. *Engineering classification of rock mass for design of tunnel support.* Rock Mechanics 6, 4, 189-236.

Dassault Systemes Inc., 2012. *ABAQUS/Standard 6.12-2.* User's Manual, RI, USA.

DIAS Engineering Inc., 2000. *GDA 1.0 Geomechanical Design Analysis Software.* User's Guide,Sudbury. ON, Canada.

Diavik Dialogue, (2011). Diavik Diamond Mine Inc., Volume 14, 4th quarter, pp:1-8.

Hadjigeorgiou J., Leclair J.G., Potvin Y., 1995. *An updated of the stability graph method for open stope desing.* 97th CIM-AGM, Rock Mechanics and Strata Control Session, Halifax, Nova Scotia.

Martin C.D., Tannant D.D., Yazici S., Kaiser P.K., 1999. *Stress path and instability around mine openings.* 9th ISRM congress, Paris, 25-28.

Mathews K.E., Hoek E., Wyllie D.C., Stewart S.B.V., 1981. *Prediction of stable excavation spans for mining at depths below 1000m in hard rock.* CANMET Report DSS Serial No. OSQ80-00081.

Mawdesley C., Trueman R., Whiten W., 2001. *Extending the Mathews stability graph for open-stope design.* Trans. Instn Min. Metall (Sect. A: Min. Techno)110, A27-A39.

Nickson S.D., 1992. *Cable support guidelines for underground hard rock mine operations, Master of Applied Science thesis.* Department of Mining and Mineral Process Engineering, University of British Columbia.

Potvin Y., 1988. *Empirical open stope design in Canada.* Ph.D. thesis, Department of Mining and Mineral Process Engineering, University of British Columbia.

Rocscience Inc., 2016. *DIPS 7.0.* Toronto, ON, Canada.

Steward S.B.V., Forsyth W.W., 1995. *The Mathews method for open stop design,* CIM Bull. 88, 45-53.

Suorineni F.T., 2010. *The stability graph after three decades in use: Experience and the way forward.* International journal of mining, Reclamation and Environment 24, 4, 307-339.

Trueman R., Mikula P., Mawdesley C., Haries N., 2000., *Experience in Australia with the application of the Mathews method of open stope desing.* CIM Bull. 93. 162-167.

Wang J., Milne D., Wegner L., Reeves M., 2006. *Numerical evaluation of the effects of stress and excavation surface geometry on the zone of relaxation around open stope hanging walls.* International Journal of Rock Mechanics and Mining Sciences 44, 289-298.